Stabilization characteristics of user load equipped with electric spring for various types of line impedance

Stefano Giacomuzzi[1], *Student Member, IEEE*, Giuseppe Buja[1], *Life Fellow, IEEE*, Qingsong Wang[2], *Senior Member, IEEE*, and Manuele Bertoluzzo[1,3]

[1]Department of Industrial Engineering, University of Padova, Padova, Italy; stefano.giacomuzzi@phd.unipd.it, giuseppe.buja@unipd.it, manuele.bertoluzzo@unipd.it, [3]corresponding author

[2]School of Electrical Engineering, Southeast University, Nanjing, China; qswang@seu.edu.cn

***Abstract*—In the last years, Renewable Energy Sources (RESs) have increasingly contributed to the power delivered by the grid. Despite the environmental benefits made by RESs, their unpredictable power production is responsible of variations in the voltage of the distribution lines that can be disruptive for the functioning of the supplied loads. Electric Spring (ES) is a device that faces such an issue by stabilizing the supply voltage of the critical load of a user in a simple but effective way. This paper is concerned with the stabilization characteristics of a user load supplied by a low-voltage distribution line and equipped with a reactive power-operated ES. After working out an ES model that facilitates the analysis of an ES-equipped user load, its stabilization characteristics are found for three types of line impedance, namely pure resistive, pure inductive and resistive-inductive. Comparison of the resultant characteristics shows the different performance of the ES-equipped user load under various types of line impedance.**

Keywords—Electric Spring, Renewable Energy Sources, Line Impedance, Voltage Stabilization.

I. INTRODUCTION

Proliferation of Renewable Energy Sources (RESs) is driven by the need of cutting the polluting emissions of the conventional power stations and, at the same time, to support them in fulfilling the increasing electric power demand. On the other side, the unpredictable and/or intermittent RES power production is an issue for the steady operation of the grid because it can give rise to some mismatch between power generation and demand. As a result, the quality of the service of the electric system further to the RES proliferation experiences ups and downs [1]. The benefit is related to their distributed allocation that reduces the voltage drop along the distribution lines. On the other hand, an unpredicted shortage of their power production yields an undervoltage in the distribution lines; an equally undesired situation occurs when there is an excess of power production from RESs, yielding an overvoltage in the distribution lines.

Electric Spring (ES) is a device that faces the variations of the supply voltage of a user load in a simple but effective way. The basic concepts behind the ES application are as follows:

- to divide the user load into two groups: one has to be supplied with a voltage close to the nominal one to meet the requirements and is termed Critical Load (CL); the other one tolerates a large variation of the supply voltage and is termed Non-Critical Load (NCL),
- to decrease or increase the power absorbed by NCL according to whether there is a shortage or an excess of the power delivery from RESs so as to keep constant the power absorbed by CL and, with it, to stabilize the CL supply voltage [2]-[3],
- to entrust ES with the task of adjusting the absorption of power from NCL.

Fig. 1 illustrates the schematics of a single-phase user load connected to a Low Voltage (LV) distribution line and equipped with ES. ES consists of a voltage source inverter (VSI), filtering inductor L_f and capacitor C, which acts as the load for VSI and is interposed between the LV distribution line and NCL. The series of ES and NCL as well as CL are connected in parallel at the same point of the LV distribution line, commonly called as point of common coupling (PCC). The set formed by ES and NCL is termed Smart Load (SL) and constitutes the key stage of the ES-equipped user load since it adjusts the power absorbed by NCL to keep constant that one absorbed by CL. Other quantities in Fig. 1 are: voltage V_{DC}, which represents the voltage of a DC source at the ES input, voltage v_{ES}, which is the ES output voltage, voltage v_{NCL}, which is the NCL voltage, and voltage v_S, which is the PCC voltage and coincides with the CL supply voltage.

ES stabilizes the magnitude of v_S by adjusting v_{ES} under the government of a local control system. Its ability of stabilizing V_S without requiring any communication to a grid monitor empowers ES as a major tool for the voltage stabilization along the distribution lines, specifically of the critical load of the users [4], [5]. This explains the intensive research activities that have been carried out in recent times on ES, leading to the proposal of several ES versions with various topologies and control methods. Depending on the DC source at the ES input, the versions are basically two: one utilizes a capacitor as DC source; this entails that ES puts at stake only reactive power to stabilizes V_S [6], [7]; the other one utilizes a power supply (a battery pack or a grid-supplied

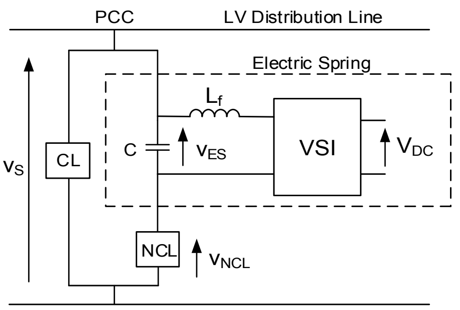

Fig. 1. Schematic of a single-phase ES-equipped user load.

capacitor) as DC source, thus giving ES the capability to put at stake both reactive and active power [8], [9]. The latter version makes ES able to execute ancillary services (in addition to the stabilization of V_S) in favor of both the user and the grid, such as power factor correction and frequency support [10], [11]. In return, the relevant ESs have a more complex structure and control scheme [12]-[14].

In the LV distribution lines, the section of the conductors is notably shrunken with respect to the high/medium-voltage transmission/distribution lines. At first glance, it should follow that the resistive component of the impedance of the LV distribution lines predominates over the reactive one. In practice, the following matters play also a role in determining the impedance of a LV distribution line: i) the output impedance of the MV/LV transformer; it is mainly inductive and contributes to the impedance seen by a user connected to a LV distribution line, ii) the length of the LV distribution line; indeed, the impedance of long conductors can surmount that one of the MV/LV transformer, iii) the power to be transported; if the LV distribution line is committed to the delivery of high powers, its conductors are sized with a larger section, thus lowering their resistive component, and iv) the placement (underground or overhead) of the LV distribution line; indeed, the overhead conductors have a lower resistance/reactance ratio compared to the cables. Therefore, as a general rule, it can be stated that the impedance of the LV distribution lines is i) prevalently resistive for long cables, which is a situation quite common in Europe, ii) prevalently reactive for short overhead lines, and iii) in between the two situations for intermediate line arrangements.

This paper refers to a reactive power-operated ES that stabilizes the CL supply voltage of a user connected to a single-phase LV distribution line. The aim of the paper is to investigate the stabilization characteristics of an ES-equipped user load under different LV line impedance cases. Organization of the paper is as follows. Section II describes circuitry and operation of an ES-equipped user load. Section III analyzes the SL operation for a resistive and a resistive-inductive NCL, hereafter designated with R-NCL and RL-NCL respectively. Section IV formulates the stabilization characteristics for the two extreme types of LV distribution line: pure resistive and pure inductive, hereafter designated with R-line and L-line, respectively. Section V extends the examination of the stabilization characteristics to a line with resistive-inductive impedance, designated with RL-line. Section VI concludes the paper. Appendix reports the data of the case study examined in the paper.

Throughout the paper i) AC voltages and currents are sinusoidal, ii) lower-case and upper-case letters denote time-variables and specific quantities, respectively, like magnitudes of sinusoidal variables and circuitry parameters, and iii) an upper-case letter with a bar or a point on denotes a phasor or an impedance, respectively.

II. ES-EQUIPPED USER LOAD DESCRIPTION

Let us consider a single-phase ES-equipped user load with a reactive power-operated ES. Its circuital diagram is drawn in Fig. 2, where v_G and i_G are the voltage applied to the LV distribution line by the grid and the current absorbed by the user from the line; v_S and i_{CL} are the CL voltage and current; i_{NCL} is the NCL current; v_{VSI} is the VSI output voltage; i_I is the ES output current, i_C is the current flowing into C; R_{CL} and L_{CL}, R_{NCL} and L_{NCL} are the resistances and inductances of CL and NCL, respectively; C_{DC} is the capacitor at the ES input. For the LV distribution line, a generic impedance composed by resistance R_G and inductance L_G is drawn.

In the diagram of Fig. 2, the fluctuations of the power generated by RESs deviate V_G from its nominal value $V_{G,N}$ and this, in turn, produces the variation of V_S from its nominal value $V_{S,N}$.

The time-domain equations of the circuital diagram in Fig. 2 are

$$\begin{cases} v_S = v_{ES} + v_{NCL} \\ v_G - v_S = R_G i_G + L_G \frac{di_G}{dt} \\ i_C = i_I + i_{NCL} \\ i_G = i_{CL} + i_{NCL} \end{cases} \tag{1}$$

where the voltages across CL, NCL and C are expressed as follows:

$$\begin{aligned} v_S &= R_{CL} i_{CL} + L_{CL} \frac{di_{CL}}{dt} \\ v_{NCL} &= R_{NCL} i_{NCL} + L_{NCL} \frac{di_{NCL}}{dt} \\ v_{ES} &= \frac{1}{C} \int i_C \, dt \end{aligned} \tag{2}$$

Current i_I must either lead or lag v_{ES} of $\pi/2$ for ES to exchange only reactive power. Since current i_C through C is always leading v_{ES} of $\pi/2$, current i_I must be either in phase with or in opposition to i_{NCL}, and voltage v_{ES} is in quadrature with i_{NCL}.

When V_G is equal to $V_{G,N}$, CL is properly supplied and voltage v_{ES} is kept at zero; this is obtained by forcing i_I to have the same magnitude as and the opposite phase of i_{NCL} (i.e. by forcing i_I to be equal to $-i_{NCL}$) so that i_C is zero. Under this circumstance, NCL is also supplied at the nominal voltage. When V_G deviates from $V_{G,N}$, ES stabilizes the CL voltage at $V_{S,N}$ by suitably adjusting the magnitude of V_{ES}. The adjustment is obtained by means of a control system that senses and manipulates V_S so as to command the injection of current i_I of appropriate magnitude into C while keeping its phase equal or opposed to that of i_{NCL}. Convenient design of ES keeps i_I in opposition to i_{NCL}.

III. SL OPERATION

Operation of SL and, later on, of an ES-equipped user load is analyzed under the following assumptions:

- variables are in steady-state,
- voltage V_S is stabilized at $V_{S,N}$.

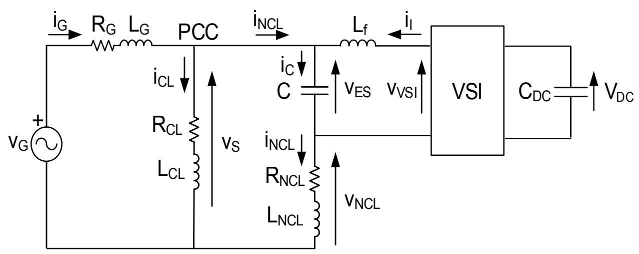

Fig. 2. Circuital diagram of a single-phase ES-equipped user load.

A reactive power-operated ES can work in two modes: capacitive or inductive. It works in the capacitive mode when $\bar{I}_{NCL}$ leads $\bar{V}_{ES}$ by π/2, and in the inductive mode when $\bar{I}_{NCL}$ is lagging $\bar{V}_{ES}$ by π/2. In the phasor domain, the third relationship in (1) can be rewritten as

$$\bar{I}_C = \left(1 + \frac{\bar{I}_I}{\bar{I}_{NCL}}\right) \bar{I}_{NCL} \tag{3}$$

Being currents $\bar{I}_I$ and $\bar{I}_{NCL}$ in phase opposition, ratio $\bar{I}_I/\bar{I}_{NCL}$ is a real negative number that ranges from 0 to a value less than -1, being equal to -1 at the nominal grid voltage. Further to (3), ES can be modeled as an equivalent reactance connected in series to NCL, given by

$$X_{eq} = \left(1 + \frac{\bar{I}_I}{\bar{I}_{NCL}}\right) X_C \tag{4}$$

where $X_C = -1/(\omega C)$ and ω is the grid angular frequency. Since $\bar{V}_{ES}$ is just the voltage drop across X_{eq}, the so-called capacitive and inductive working modes of ES correspond to a negative and a positive value of X_{eq}, respectively. In particular, inequality $(\bar{I}_I/\bar{I}_{NCL}) < -1$ establishes the condition for ES to work in the inductive mode.

The change of X_{eq} because of the ES operation modifies the other SL quantities as follows. The NCL current becomes

$$\bar{I}_{NCL} = \frac{\bar{V}_{S,N}}{[R_{NCL} + j(X_{NCL} + X_{eq})]} \tag{5}$$

and the voltages across C and NCL modify accordingly

$$\bar{V}_{ES} = jX_{eq}\bar{I}_{NCL} \tag{6a}$$

$$\bar{V}_{NCL} = (R_{NCL} + jX_{NCL})\bar{I}_{NCL} \tag{6b}$$

Voltage V_{NCL} for both R-NCL and RL-NCL is plotted in Fig. 3 (a) as a function of X_{eq} and in Fig. 3 (b) as a function of V_{ES}, where positive values are assigned to V_{ES} for ES working in the capacitive mode, and negative values in the inductive mode. The curves of Figs. 3 refer to the data of the case study reported in Appendix and are plotted for nominal voltage $V_{S,N}$ equal to 230 V. Voltages V_{NCL} and V_{ES} in Figs. 3 are normalized to $V_{S,N}$ whilst X_{eq} is given as a fraction of X_C.

The curves of Figs. 3 show that, when ES works in the inductive mode, voltage V_{NCL} is less than $V_{S,N}$ irrespectively of NCL. Instead, when ES works in the capacitive mode, voltage V_{NCL} is always less than $V_{S,N}$ for R-NCL whilst it exceeds $V_{S,N}$ for RL-NCL. This can be readily explained by substituting (5) in (6b) and by rewriting the result in the magnitude form

$$V_{NCL} = \frac{|R_{NCL} + jX_{NCL}|}{|R_{NCL} + j(X_{NCL} + X_{eq})|} V_{S,N} \tag{7}$$

By (7), reactance X_{NCL} is 0 and V_{NCL} is always less than $V_{S,N}$ for R-NCL. Conversely, voltage V_{NCL} can be greater than $V_{S,N}$ only if $X_{NCL}>0$ for RL-NCL. Moreover, it can be observed from (7) that V_{NCL} exceeds $V_{S,N}$ when $-2X_{NCL} < X_{eq} < 0$, i.e. when ES works in the capacitive mode, as anticipated above. The maximum value reached by V_{NCL} is achieved for $X_{eq}=-X_{NCL}$ and is correlated to the power factor of NCL as

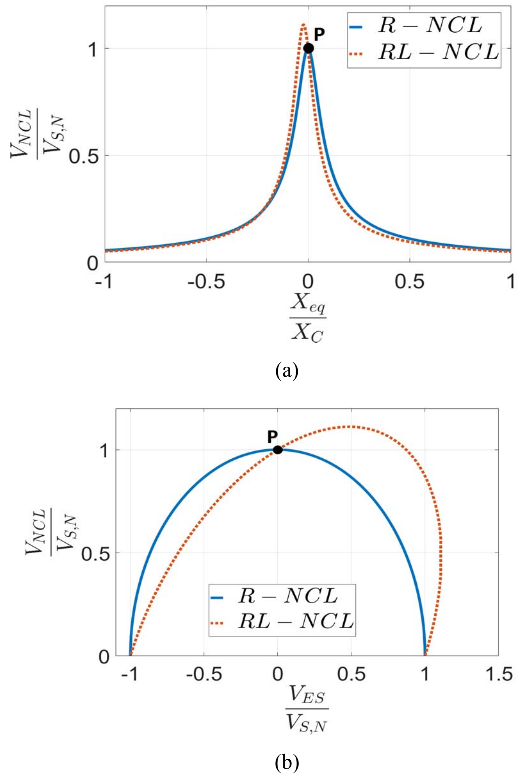

Fig. 3. V_{NCL} as a function of (a) X_{eq} and (b) V_{ES} for R-NCL (solid blue line) and RL-NCL (dotted red line).

$$V_{NCL,max} = \frac{V_{S,N}}{\cos \varphi_{NCL}} \tag{8}$$

Note that, when $X_{eq}<-X_{NCL}$, the capacitance of X_{eq} prevails over the inductance of X_{NCL} and SL exhibits a resistive-capacitive behavior.

The curves of Figs. 3 are distinctive of the SL operation since they depend only on its parameters and the ES output current, while they are not depending on the line impedance [15]. Conversely, the operating point of SL depends of the line impedance. Specifically, at the nominal grid voltage, SL operates at point P in Figs. 3 whilst, in the presence of a grid voltage variation, the SL operating point shifts along the curves and settles at a point fixed by the line impedance.

IV. ES-EQUIPPED USER LOAD STABILIZATION CHARACTERISTICS

This Section and the next one investigate the impact of the impedance type of a LV distribution line on the stabilization characteristics of an ES-equipped user load. The cases of a pure R-line and a pure L-line are here discussed whilst the next Section discusses the case of an RL-line. To do an all-case investigation, only RL-NCL is considered, whereby the characteristics of R-NCL can be readily deduced from those of RL-NCL by putting $X_{NCL}=0$ in the equations describing the SL operation.

A. R-line

The grid voltage gets nominal value $V_{G,N}$ when the CL voltage is equal to $V_{S,N}$ and V_{ES} is zero. In the phasor form, voltage $V_{G,N}$ is expressed as

$$\bar{V}_{G,N} = \left[1 + R_G\left(\frac{1}{R_{CL}+jX_{CL}} + \frac{1}{R_{NCL}+jX_{NCL}}\right)\right]\bar{V}_{S,N} \quad (9)$$

When the grid voltage varies and the CL voltage is stabilized at $V_{S,N}$, the relationship between $\bar{V}_G$ and $\bar{V}_{G,N}$ can be written as

$$\bar{V}_G = \frac{1+R_G\left(\frac{1}{R_{CL}+jX_{CL}}+\frac{1}{R_{NCL}+j(X_{NCL}+X_{eq})}\right)}{1+R_G\left(\frac{1}{R_{CL}+jX_{CL}}+\frac{1}{R_{NCL}+jX_{NCL}}\right)}\bar{V}_{G,N} \quad (10)$$

By manipulating (5), (6), (9) and (10), and by extracting V_{NCL} and V_{ES} as a function of V_G, the curves of Fig. 4 (a) are obtained. In the figure, voltages V_{NCL} and V_{ES} as well as V_G are given in terms of variation from the respective values at the nominal grid voltage, and are expressed as a percentage of $V_{S,N}$ and $V_{G,N}$, respectively. In formula, it is

$$\Delta V_{NCL\%} = \frac{V_{NCL}-V_{S,N}}{V_{S,N}}\cdot 100 \quad (11)$$

$$\Delta V_{ES\%} = \frac{V_{ES}-V_{ES,N}}{V_{S,N}}\cdot 100 \equiv \frac{V_{ES}}{V_{S,N}}\cdot 100 \quad (12)$$

$$\Delta V_{G\%} = \frac{V_G-V_{G,N}}{V_{G,N}}\cdot 100 \quad (13)$$

where $V_{ES,N}$ is 0. The curves of Fig. 4 (a) reveal that an ES-equipped user load has the following stabilization characteristics with an R-line:

- there is a maximum grid overvoltage that ES is able to stabilize; it is 2% of $V_{G,N}$ for the case study. In correspondence, ES works in the capacitive mode with V_{ES} of about 0.5×230 V (point 2_R in the figure),
- minimum grid undervoltage is limited by the fact that V_{NCL} reduces to zero; this occurs for an undervoltage of about -10% (point 3_R). In correspondence, ES works in the inductive mode with V_{ES} equal to 230 V,
- the curves of V_{ES} and V_{NCL} have two stretches in the grid voltage stabilization range; this means that there are two possible operating points of the ES-equipped user load. Looking at the V_{ES} curve, one stretch goes from point 3_R to 2_R, and the other one goes from point 2_R to 6_R. Looking at the V_{NCL} curve, the two stretches are almost overlapping,
- at nominal grid voltage, the values of V_{ES} at the two operating points are 0 V (point 4_R) and 0.8×230 V (point 5_R), and the corresponding values of V_{NCL} are around 230 V. To better appreciate the V_{NCL} values, the curves of Fig. 4 (a) are magnified in Fig. 4 (b) around the nominal grid voltage; from them it turns out that V_{NCL} is equal to 230 V for V_{ES}=0 V, as expected, while it is a little greater than 230 V (of about 1%) for the other value of V_{ES},
- in a reasonable range of stabilization of the grid voltage, which goes from 2% down to -5% (corresponding to a V_{NCL} drop of about 30%), voltage V_{ES} takes smaller values if the operating point stays on the stretch that goes from point 3_R to 2_R; therefore, it is convenient to operate ES along this stretch to reduce the voltage stress across C, and this goal can be achieved by a suitable command of the ES output current.

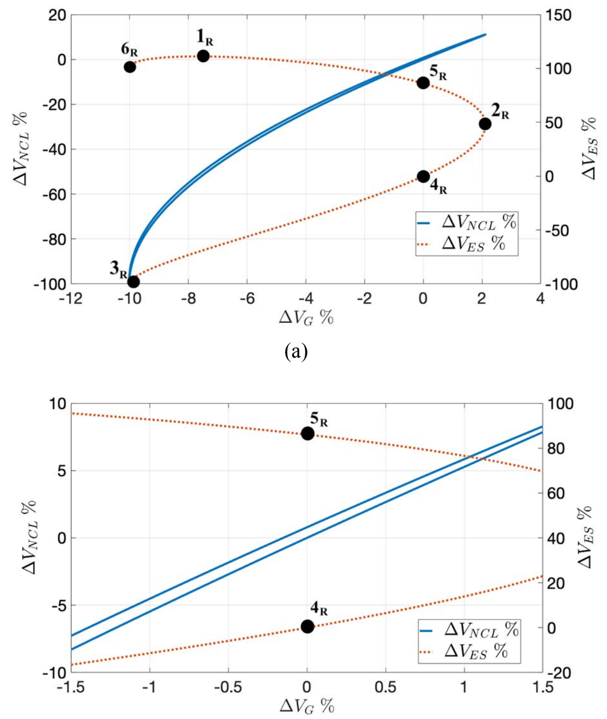

(a)

(b)

Fig. 4. (a) ΔV_{NCL} (solid blue line) and ΔV_{ES} (dashed red line) as a function of ΔV_G for an R-line, and (b) magnification of the curves in (a) around $V_{G,N}$.

B. L-line

For an L-line the nominal grid voltage is expressed as

$$\bar{V}_{G,N} = \left[1 + jX_G\left(\frac{1}{R_{CL}+jX_{CL}} + \frac{1}{R_{NCL}+jX_{NCL}}\right)\right]\bar{V}_{S,N} \quad (14)$$

When the grid voltage varies and the CL voltage is stabilized at $V_{S,N}$, the relationship between $\bar{V}_G$ and $\bar{V}_{G,N}$ can be written as

$$\bar{V}_G = \frac{1+jX_G\left(\frac{1}{R_{CL}+jX_{CL}}+\frac{1}{R_{NCL}+j(X_{NCL}+X_{eq})}\right)}{1+jX_G\left(\frac{1}{R_{CL}+jX_{CL}}+\frac{1}{R_{NCL}+jX_{NCL}}\right)}\bar{V}_{G,N} \quad (15)$$

By manipulating (5), (6), (14) and (15), and by extracting V_{NCL} and V_{ES} as a function of V_G, as previously done for an R-line, the curves of Fig. 5 are obtained. They are calculated for a line reactance equal to the resistance of the R-line case (i.e. equal to 2 Ω). Voltages V_{NCL}, V_{ES} and V_G in the graphs of the figure are still given by (11)-(13).

The curves of Fig. 5 reveal that an ES-equipped user load has the following stabilization characteristics with an L-line:

- there is a maximum grid overvoltage that ES is able to stabilize; it is 0.9% of $V_{G,N}$ for the case study. In correspondence, ES works in the inductive mode with V_{ES} of 0.3×230 V (point 3_L in the figure) and a drop of V_{NCL} of 0.17×230 V (point 7_L),
- there is also a minimum grid undervoltage that ES is able stabilize; it is -12% of $V_{G,N}$ for the case study. In correspondence, ES works in the capacitive mode with V_{ES} of 1.06×230 V (point 2_L) and a V_{NCL} drop of 0.25×230 V

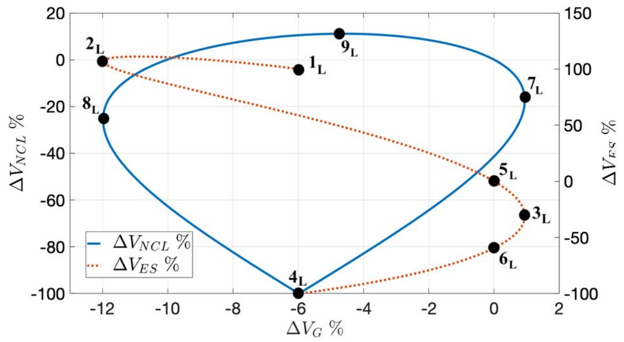

Fig. 5. ΔV_{NCL} (solid blue line) and ΔV_{ES} (dashed red line) as a function of ΔV_G for an L-line.

(point 8_L),

- the curves of V_{ES} and V_{NCL} have two stretches in the grid voltage stabilization range; this means that there are two possible operating points of the ES-equipped user load. Looking at the V_{ES} curve, one stretch goes from point 3_L to 2_L, whilst the other one is made of two pieces: one piece goes from point 4_L to 3_L and the other piece goes from point 2_L to 1_L. Looking at the V_{NCL} curve, one stretch goes from point 7_L to 8_L passing through point 9_L and is associated to the stretch 3_L-2_L of the V_{ES} curve, and the other one goes from point 7_L to 8_L passing through point 4_L and is associated to the stretch 4_L-3_L of the V_{ES} curve. Note that along the central part of the V_{NCL} stretch passing through point 9_L, voltage V_{NCL} exceeds 230 V; in particular, at point 9_L, it reaches the maximum value of 255 V, as predicted by (8),

- at nominal grid voltage, the magnitudes of V_{ES} at the two operating points are 0 V (point 5_L) and 0.6×230 V (point 6_L); the corresponding values of V_{NCL} are respectively 230 V, as expected, and 140 V, with a drop of about 40%,

- in the grid voltage stabilization range, voltage V_{ES} takes smaller values if the operating point stays on the stretch that goes from point 3_L to 2_L rather than in the other stretch; furthermore, V_{NCL} varies around 230 V along the former stretch. Therefore, by a suitable command of the ES output current, it is convenient to operate ES along this stretch both to reduce the voltage stress across C and to supply NCL with a voltage close to the nominal one.

C. Discussion

A comparison of the results found for an R-line and an L-line underlines that

- in both cases, the voltage stabilizing action of ES is stronger under grid undervoltage rather than under overvoltage conditions,

- the maximum grid overvoltage that ES is able to stabilize is higher for an R-line,

- the minimum grid undervoltage that ES is able to stabilize is limited for an L-line, whilst it is dictated only by the zeroing of V_{NCL} for an R-line,

- the ES working mode under grid overvoltages as well as under grid undervoltages depends on the type of line impedance, as it can be recognized from the phasor diagrams of Fig. 6. Under grid overvoltages, the ES working mode is capacitive with an R-line and inductive with an L-line; under grid undervoltages, the ES working mode is inductive with an R-line and capacitive with an L-line.

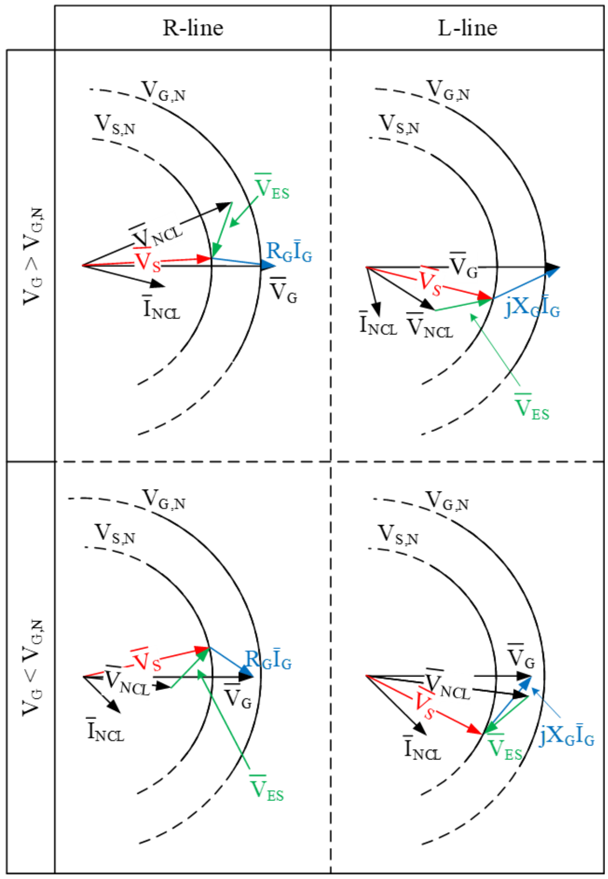

Fig. 6. Phasor diagrams of ES-equipped user load under grid undervoltage and overvoltage conditions for an R-line and an L-line.

V. RL-LINE

The stabilization characteristics of an ES-equipped user load are here investigated for an RL-line with resistance R_G equal to reactance X_G, and line impedance Z_G equal to that one of the two cases dealt with in the previous Section (i.e. equal to 2 Ω). From the equations describing the operation of the ES-equipped user load with this type of line, the curves of Fig. 7 are obtained. Voltages V_{NCL}, V_{ES} and V_G in the figure are still given by (11)-(13).

The curves of Fig. 7 point out similarities and differences of the stabilization characteristics of the ES-equipped user load with an RL-line compared to those with an R-line and RL-line:

- the V_{NCL} and V_{ES} curves are more similar to those with an L-line, being their shape slightly different. The curves maintain two stretches so that there are again two possible operating points for the ES-equipped user load,

- the maximum grid overvoltage that ES is able to stabilize is 0.1% of $V_{G,N}$, which is quite less than with an L-line but much less than with an R-line. The minimum grid undervoltage that ES is able to stabilize is the same as with an L-line, i.e. of -12% $V_{G,N}$. From these outcomes, it can be inferred that the line resistance notably reduces the

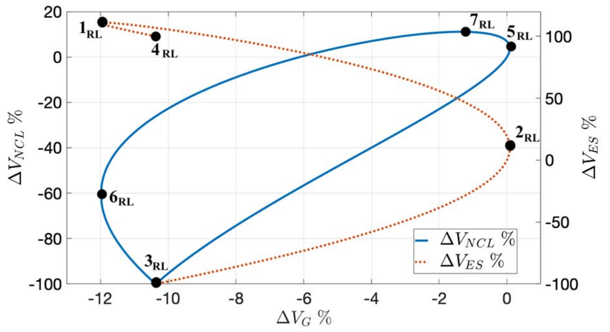

Fig. 7. ΔV_{NCL} (solid blue line) and ΔV_{ES} (dashed red line) as a function of ΔV_G for an RL-line with $R_G = X_G$.

stabilization capabilities under grid overvoltages while it does not affect those under grid undervoltages,

- as with an L-line, it is convenient to operate along the V_{ES} stretch that goes from point 2_{RL} to 1_{RL} since, in correspondence, V_{NCL} goes from 5_{RL} to 6_{RL} and NCL is supplied at a higher voltage. However, for this type of line, the V_{NCL} drop in the grid voltage stabilization range is greater than with an L-line as it is of 60% for ΔV_G=-12% (point 6_{RL}). Another peculiarity of the V_{NCL} curve is the part of the stretch that exceeds 230 V; under grid overvoltages, it extends up to point 5_{RL}, where V_{NCL} is equal to 1.04×230 V, whilst the maximum of V_{NCL} remains equal to 255 V, according to (8), and is reached at point 7_{RL}.

VI. CONCLUSIONS

A comprehensive investigation of the behavior of a user load connected to an LV distribution line and equipped with a reactive power-operated ES has been carried out for different types of line impedance. The main conceptual finding ensuing from the investigation is that there are two players that determine the behavior of an ES-equipped user load, including its stabilization capabilities; they are SL and the type of line impedance. This entails that SL must be tailored to the type of line impedance in order to get the best benefit from the use of ES.

Apart from the finding above, the paper has examined in detail the stabilizing characteristics of an ES-equipped user load by formulating the equations of the voltages across NCL and ES, and by determining the grid voltage stabilization range for three types of impedance of the LV distribution line supplying the user, namely R, L and RL. As an exemplification, curves and numerical values are given for the stabilization characteristics of a case study of ES-equipped user load.

APPENDIX

The data of the ES-equipped user load utilized as a case study are listed in Table I. Throughout the paper, CL is an RL impedance with cosφ=0.9 whilst for NCL the two cases of an R and an RL impedance, still with cosφ=0.9, have been examined. Among the data, it is worth to note that the nominal active power absorbed by NCL has been put greater than that of CL, with a ratio of 3 between the twos.

TABLE I. CASE STUDY DATA

Nominal Grid Voltage with R-line ($V_{G,N}$)	265 V
Nominal Grid Voltage with RL-line ($V_{G,N}$)	267 V
Nominal Grid Voltage with L-line ($V_{G,N}$)	249 V
CL Nominal Voltage ($V_{S,N}$)	230 V
CL Nominal Active Power (P_{CL})	1 kW
CL Power Factor ($\cos\varphi_{CL}$)	0.9
CL Resistance (R_{CL})	42.8 Ω
CL Reactance (X_{CL})	20,7 Ω
NCL Nominal Active Power (P_{NCL})	3 kW
NCL Power Factor ($\cos\varphi_{CL}$)	0.9
NCL Resistance (R_{NCL})	14.3 Ω
NCL Reactance (X_{NCL})	6,92 Ω
LV Distribution Line Impedance (Z_G)	2 Ω
ES Capacitor (C)	10 µF

REFERENCES

[1] M. Bollen, "The Smart Grid – Adapting the power system to new challenges", Synthesis Lecturers on Power Electronics, Series Editor: Jerry Hudgins, Morgan & Claypool Publishers, Chapter 2, 2011.

[2] S. Y. R. Hui, C. K. Lee, and F. F. Wu, "Electric springs—a new smart grid technology," *IEEE Trans. on Smart Grid*, vol. 3, no. 3, pp. 1552–1561, Sep. 2012.

[3] C. K. Lee, S. C. Tan, F. F. Wu, S. Y. R. Hui and B. Chaudhuri, "Use of Hooke's law for stabilizing future smart grid — The electric spring concept," in Proc. of Energy Convers. Conf. & Expo., 2013, pp. 5253-5257.

[4] Y. Yang, S. S. Ho, S. C. Tan, and S. Y. R. Hui, "Small-signal model and stability of electric springs in power grids," *IEEE Trans. on Smart Grid*, vol. 9, no. 2, pp. 857–865, Mar. 2018.

[5] X. Luo *et al.*, "Distributed voltage control with electric springs: Comparison with STATCOM," *IEEE Trans. on Smart Grid*, vol. 6, no. 1, pp. 209–219, Jan. 2015.

[6] N. R. Chaudhuri, C. K. Lee, B. Chaudhuri and S. Y. R. Hui, "Dynamic Modeling of Electric Springs," *IEEE Trans. on Smart Grid*, vol. 5, no. 5, pp. 2450-2458, Sept. 2014.

[7] D. Chakravorty, J. Guo, B. Chaudhuri, and S. Y. R. Hui, "Small Signal Stability Analysis of Distribution Networks with Electric Springs," *IEEE Trans. on Smart Grid*, vol. 10, no. 2, pp. 1543-1552, Mar. 2019.

[8] S. Tan, C. K. Lee and S. Y. Hui, "General Steady-State Analysis and Control Principle of Electric Springs With Active and Reactive Power Compensations," *IEEE Trans. on Power Electron.*, vol. 28, no. 8, pp. 3958-3969, Aug. 2013.

[9] Q. Wang, M. Cheng, Y. Jiang, W. Zuo and G. Buja, "A Simple Active and Reactive Power Control for Applications of Single-Phase Electric Springs," *IEEE Trans. Ind. On Electron.*, vol. 65, no. 8, pp. 6291-6300, Aug. 2018.

[10] J. Soni and S. K. Panda, "Electric Spring for Voltage and Power Stability and Power Factor Correction," *IEEE Trans. on Ind. App.*, vol. 53, no. 4, pp. 3871-3879, July-Aug. 2017.

[11] X. Chen, Y. Hou, S. C. Tan, C. K. Lee, and S. Y. R. Hui, "Mitigating voltage and frequency fluctuation in microgrids using electric springs," *IEEE Trans. Smart Grid*, vol. 6, no. 2, pp. 508–515, Mar. 2015.

[12] Q.Wang, F.Deng, M.Cheng and G.Buja, "The State of the Art of Topologies for Electric Springs", *MDPI Journal on Energies*, Vol. 11, no. 7, pp. 1-21, July 2018.

[13] Q. Wang, P. Chen, F. Deng, M. Cheng and G. Buja, "The State of the Art of the Control Strategies for Single-Phase Electric Springs," *MDPI Journal on Applied Sciences*, vol. 8, no. 2019, pp. 1-13, Oct. 2018.

[14] K. T. Mok, S. C. Tan, and S. Y. R. Hui, "Decoupled power angle and voltage control of electric springs," *IEEE Trans. on Power Electron.*, vol. 31, no. 2, pp. 1216–1229, Feb. 2016.

[15] C. K. Lee, K. L. Cheng and W. M. Ng, "Load characterization of electric spring," 2013 in Proc. of IEEE Energy Convers. Congr. Expo., 2013, pp. 4665-4670.